Methods 204 (2022) 160–171

Contents lists available at ScienceDirect

Methods

journal homepage: www.elsevier.com/locate/ymeth

Determining translocation orientations of nucleic acid helicases

Himasha M. Perera, Michael A. Trakselis *

Department of Chemistry and Biochemistry, Baylor University, Waco, TX 76798, USA

ARTICLE INFO

Keywords:
DNA replication
MCM helicase
Translocation
Unwinding
Polarity
Orientation

ABSTRACT

Helicase enzymes translocate along an RNA or DNA template with a defined polarity to unwind, separate, or remodel duplex strands for a variety of genome maintenance processes. Helicase mutations are commonly associated with a variety of diseases including aging, cancer, and neurodegeneration. Biochemical characterization of these enzymes has provided a wealth of information on the kinetics of unwinding and substrate preferences, and several high-resolution structures of helicases alone and bound to oligonucleotides have been solved. Together, they provide mechanistic insights into the structural translocation and unwinding orientations of helicases. However, these insights rely on structural inferences derived from static snapshots. Instead, continued efforts should be made to combine structure and kinetics to better define active translocation orientations of helicases. This review explores many of the biochemical and biophysical methods utilized to map helicase binding orientation to DNA or RNA substrates and includes several time-dependent methods to unequivocally map the active translocation orientation of these enzymes to better define the active leading and trailing faces.

1. Introduction and classifications of helicases/translocases

An essential requirement for efficient DNA replication is the enzyme-catalyzed DNA unwinding by replicative helicases, which act as a lynchpin for the replisome to control assembly, progression, and termination. Despite the ever-increasing body of research, there is substantial disparity over the precise molecular mechanisms involving DNA unwinding, particularly, regarding the helicase ring orientation on DNA during active unwinding. While extensive experimentation has been carried out to interpret the static binding orientations of helicases on DNA, there is a need to address the translocation orientation of helicases during active unwinding. The main focus of this review is to analyze the current body of research on helicases from different organisms, compare and contrast different classifications of helicases, and examine translocation mechanisms with a specific focus on looking at methods of determining active helicase translocation orientation on DNA.

1.1. Superfamilies

Based on the characteristic features and amino acid sequence identity of conserved sequence motifs, helicases can be divided into six superfamilies (SFs) SF1-SF6 [1,2]. Members of SF1 and SF2 are defined by seven signature motifs, are generally monomeric or dimeric, and work in a variety of RNA and DNA dependent metabolism processes [3]. Although there are subtle differences between the arrangement of motifs for SF1 or SF2 helicases, they can be characterized structurally by twin core RecA domains that bind and hydrolyze NTP for energy coupled to unwinding. Relevant examples include PcrA/Rep/UvrD for SF1 and DEAD-box (*i.e.* Ded1), RecQ-like (*i.e. Ec*RecQ), or Swi/Snf2 (*i.e.* INO80) within the largest superfamily, SF2 [4,5]. Hexameric helicases fall into superfamilies SF3 through SF6 with common examples of SV40 Large T antigen (SV 40 L-Tag) and papilloma virus E1 (SF3); T4 gp41, T7 gp4, bacterial DnaB and mitochondrial Twinkle helicase (SF4); Rho (SF5); and archaeal and eukaryotic minichromosome maintenance proteins (MCMs) (SF6) (Table 1).

Abbreviations: CMG, cdc45/MCM2-7/GINS; C@duplex, CTD adjacent to the duplex; CTD, C-terminal domain; MCM, minichromosome maintenance; EM, electron microscopy; EMSA, electrophoretic mobility shift assay; FA, fluorescence anisotropy; FRET, fluorescence energy resonance energy transfer; MSE, modified steric exclusion; N@duplex, NTD adjacent to the duplex; NTD, N-terminal domain; NTP, nucleic acid triphosphate; OBD, origin binding domain; SCE, side channel extrusion; SE, steric exclusion; SEW, steric exclusion and wrapping; SF, superfamily; smFRET, single molecule fluorescence energy resonance energy transfer.

* Corresponding author.
E-mail address: michael_trakselis@baylor.edu (M.A. Trakselis).

https://doi.org/10.1016/j.ymeth.2021.11.001
Received 6 September 2021; Received in revised form 29 October 2021; Accepted 2 November 2021
Available online 7 November 2021

1.2. Monomeric vs oligomeric

Helicases can also be subdivided based on their oligomeric state. The oligomeric state of SF1 and SF2 helicases are generally considered to be monomeric or dimeric, while SF3-6 helicases are hexameric. The SF1 and SF2 helicases contain two RecA folds in one polypeptide chain, which together form an ATPase site at the domain interface [1]. SF1-2 helicases can also interact, as with the RecBCD complex, that binds dsDNA ends for coupled translocation and unwinding effectively utilizing two helicases with opposite polarities [13]. The hexameric helicases in SF3-6 have evolved from broader P- loop family of ATPases, which contain an ATPase site in each of the six subunits. While the individual evolution of RecA folds give rise to SF4 helicases, SF3 and SF6 helicases arise from an ATPase associated with a variety of cellular activities (AAA^+) clade providing and ATPase active site *in trans* between adjacent subunits [1,52–54].

1.3. Translocation

1.3.1. Polarity

The DNA double helix is defined by the two anti-parallel single strands that run in opposing directions. One of the distinct features among helicases is the polarity of their translocation and movement along an oligonucleotide [48,55,56]. Once the helicase is loaded, it can translocate in either 3′-5′ (Type A) or 5′-3′ (Type B) direction determined by the polarity of the translocating strand **(**Fig. 1**A)** [1]. The members of SF1, SF2 and SF6 contain motors that can translocate in either direction. Helicases that belong to SF1 and SF2 contain enzymes that translocate both 3′-5′ (SF1A - PcrA, Rep, UvrD) and 5′-3′ (SF1B - RecD, Dda, Pif1, Rrm3) [1]. All SF3 helicases characterized to date translocate in 3′-5′ direction, whereas SF4 and SF5 translocate 5′-3′. Several examples of characterized translocation polarity from each SF are listed in Table 1. The hexameric helicases that falls into AAA^+ family of enzymes such as SV40 Large T-antigen (SF3), papilloma Virus E1 (SF3), archaeal MCM helicase (SF6), and eukaryotic MCM2-7 helicase (SF6), translocate along the encircled leading strand in 3′-5′ direction while Rec-A family enzymes such as bacterial *Escherichia coli* (*E. coli*) DnaB (SF4), T7 gp4 (SF4) translocate along the encircled lagging strand in the 5′-3′ direction [54]. The prokaryotic RuvB is a member of the SF6 hexameric proteins [1], but it is a double-strand translocase [57], tracking with a 5′-3′ polarity on one of the strands [58].

1.3.2. Translocating/non-translocating strand

Helicases unwind DNA with a unique directionality depending on which DNA strand the enzyme interacts with most strongly and tracks along. The DNA strand that the enzyme loads onto is referred as the translocating or encircled strand (for hexameric helicases), while the complementary DNA strand is referred as non-translocating or excluded strand **(**Fig. 1**A)**. The loading or binding of a helicase onto a particular ssDNA strand combined with its propensity for unwinding polarity dictates its translocation directionality.

1.3.3. DS/SS translocation

Helicases can be further categorized based on their ability or preference to bind and translocate on ssDNA or dsDNA [1] (Table 1). When translocating along dsDNA, helicases follow closely the polarity of one DNA strand and move unidirectionally [56]. Most all SF1 enzymes translocate on ssDNA, whereas SF2 contain examples of enzymes that undergo directional translocation on both ss and dsDNA in an ATP-dependent manner. Most SF2 enzymes that translocate on dsDNA follow the track of one strand and exhibit 3′-5′ polarity [56]. The NTPase activity of the some of these dsDNA translocating enzymes is stimulated more by duplex DNA than by ssDNA [1].

Although hexameric SF4 helicases from bacteria are thought to load only onto a pre-melted origin of replication to encircle ssDNA [59–61], SF6 helicases from archaea and eukaryotes encircle dsDNA during replication initiation. SF3 eukaryotic viral helicases appear to also load on to dsDNA during initiation. However, there are indications that all SF3/4/6 helicases can translocate on dsDNA biochemically (whether they do so *in vivo* is an open question). DNA is then remodeled for the helicase to favorably encircle only one of the two strands for unwinding. Therefore, hexameric helicases have the ability to translocate along ss or dsDNA depending on the overall conformation of the hexamer and the resulting inner diameter of the central channel [62,63].

Table 1
Common helicase classifications and translocation orientations.

Helicase	Superfamily (SF)	Polarity (3′-5′ or 5′-3′)	Active oligomeric state	Preferred Translocation Substrate	Leading Face (Domain/ Motif)
PcrA	SF1A	3′-5′	Monomeric	ssDNA	2A[2,4] [6]
UvrD	SF1A	3′-5′	Mon-Dimeric[5]	ssDNA	2B[3] [7,8]
Rep	SF1A	3′-5′	Mon-Dimeric[5]	ssDNA	2B[3] [9]
Dda	SF1B	5′-3′	Monomeric	ssDNA	1B(pin)/2B(hook)[3] [10]
Pif1, Dna2	SF1B	5′-3′	Monomeric	ssDNA	1A/2B[3] [11]
RecB	SF1A	3′-5′	Monomeric	dsDNA, ssDNA	1B/Arm[3] [12,13]
RecD	SF1B	5′-3′	Monomeric	ssDNA	1B pin[3] [14]
RecBCD	SF1A/B	Both	Heterotrimer	dsDNA	B-first[3] [13]
Ded1	SF2 (DEAD)	Both	Monomeric[1]	dsRNA	- [15,16]
DHX36	SF2 (DEAD)	Both	Monomeric	ssDNA (ssRNA)	RecA2[3] [17]
eIF4A	SF2 (DEAD)	Both	Monomeric	dsRNA	- [18]
Rad54, INO80, Chd1	SF2 (Snf2)	3′-5′	Monomeric[1]	dsDNA	RecA2 (2B)[4] [19–21]
XPD	SF2 (Rad3)	5′-3′	Monomeric	ssDNA	Arch/Fe-S cluster[3] [22–25]
RecG	SF2 (RecG)	3′-5′	Monomeric	ssDNA	RecA2[3] [26,27]
PriA	SF2 (RecG)	3′-5′	Monomeric	ssDNA	RecA2 (CRR)[3] [28,29]
RecQ, BLM, WRN	SF2(RecQ)	3′-5′	Monomeric[1] [30]	dsDNA	RQC domain[3] [31–33]
RIG-I, Dicer	SF2(RIG-I)	3′-5′	Dimeric	dsRNA (ssRNA)	- [34–36]
Ski2, Mtr4, Brr2	SF2 (Ski2)	3′-5′	Monomeric	ssRNA	RecA2/Ratchet[3] [37]
Hel308	SF2 (Ski2)	3′-5′	Monomeric	ssDNA	RecA2/Ratchet (II/IV)[4] [38–40]
HCV NS3	SF2 (NS3)	3′-5′	Dimeric (Monomeric)	ssRNA, dsDNA	RecA2[3] [41 42]
SV 40 LargeT, E1	SF3	3′-5′	Hexameric	ssDNA (dsDNA)	Nterm[3] [43,44]
DnaB, T7 gp4, T4 gp41, G40P, Twinkle	SF4	5′-3′	Hexameric	ssDNA (dsDNA)	Cterm[3] [45,46]
Rho	SF5	5′-3′	Hexameric	ssRNA	Cterm[3] [47,48]
MCMs	SF6	3′-5′	Hexameric	ssDNA (dsDNA)	Nterm[4] [49–51]

[1]Adopts different oligomeric states depending on which cofactors (ATP, DNA) are bound. [2]Reeling in ssDNA. [3]Inferred translocation orientation. [4]Confirmed translocation orientation.[5]Active oligomeric state is controversial.

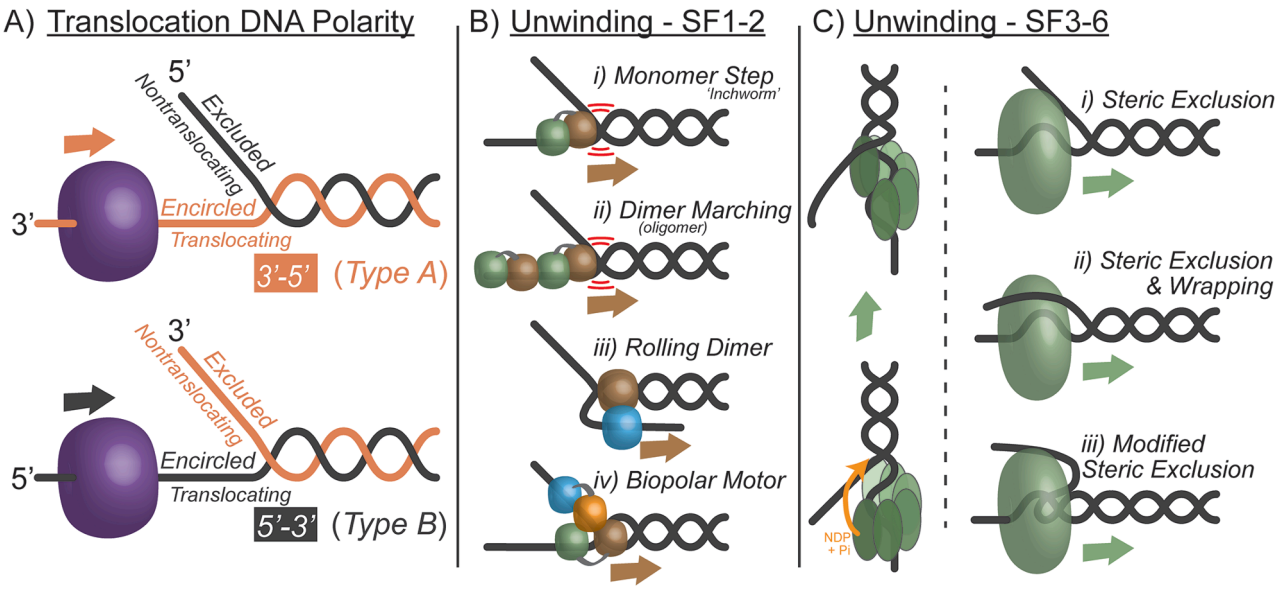

Fig. 1. Definitions of helicase translocation and unwinding. A) Shows an enzyme translocating 3′-5′ (Type A) or 5′-3′ (Type B) on the encircled or translocating strand. B) Models for unwinding for SF1-2 helicases include: i) Monomer Stepping that consists of two RecA domains that hydrolyze NTP to advance the leading domain, ii) Dimer Marching that add additional proteins to enhance the efficiency of unwinding, iii) Rolling Dimer that alternates between binding ss and dsDNA to peel off one strand, and iv) Bipolar motor that includes two helicases with opposing polarities acting on each strand. The red arcs indicate destabilization of the terminal base pair in either an active or passive fashion. C) Models for SF3-6 hand-over-hand spiral unwinding include a traditional Steric Exclusion (SE), a more nuanced Steric Exclusion and Wrapping (SEW), and a Modified Steric Exclusion (MSE) for unwinding. (For interpretation of the references to colour in this figure legend, the reader is referred to the web version of this article.)

1.3.4. Leading and trailing face

Helicase generally consist of at least two domains. This can be two RecA domains (SF1-2) or an N-terminal domain (NTD) and a C-terminal domain (CTD) (SF3-6) with each connected by a linker. Depending on the SF there can also be several subdomains or conserved motifs. Depending on which (sub)domain is at the front edge for either directional translocation or unwinding, these domains can be identified as "leading face" or "trailing face". For SF1-2 helicases with two RecA domains, RecA1 (1A) or RecA2 (2A) domain can be leading (Fig. 2). Subdomains or motifs within a single RecA domain can be used to narrow down this 'leading face' orientation more specifically (Table 1).

For a hexameric helicase that loads NTD first on to the duplex DNA (N@duplex), the leading face would be NTD and the trailing face would be CTD. Similarly, a helicase that loads CTD first on to the duplex DNA (C@duplex), will have CTD as the leading face and NTD as the trailing face (Fig. 2). While NTD or CTD can be leading or trailing faces, high-resolution structural information is required to ascertain actual and accurate leading/trailing faces during active unwinding. This is important for accurately placing and modelling interacting proteins within an unwindosome directionally with respect to translocation orientation on DNA [64,65].

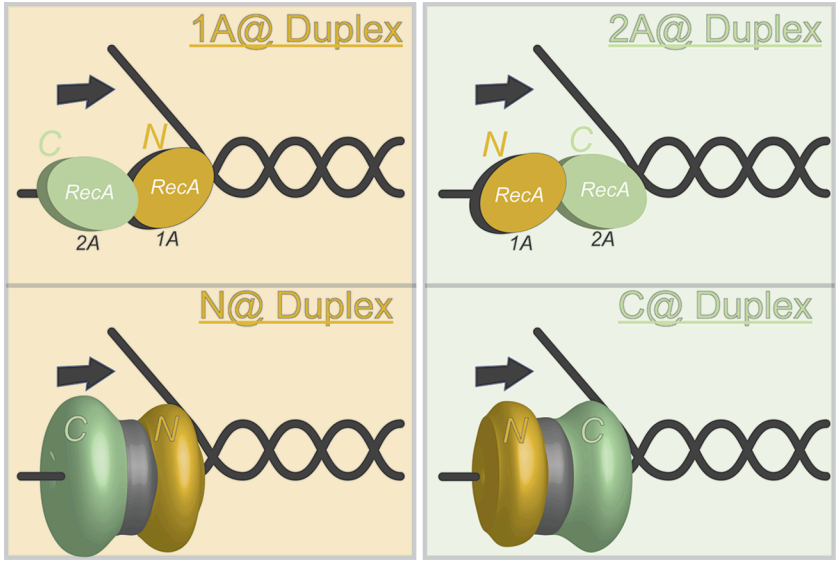

Fig. 2. Possible DNA binding orientations of monomeric or hexameric helicases. N and C are labels for the N-terminal and C-terminal domains respectively; and 1A and 2A are RecA domains in SF1 and SF2 helicases indicating relative orientations at the duplex side. Arrows indicate the direction of translocation.

1.4. Mechanisms for helicase translocation

Helicases employ different mechanisms for translocation. Monomeric helicases translocate by the well- established inchworm mechanism (Fig. 1**B**); whereas, hexameric helicases utilize a hand-over hand mechanism for translocation (Fig. 1**C**) [56]. Both mechanisms work on subunit or domain rotation powered by the NTPase cycle. The key feature that distinguishes the two mechanisms is whether the helicase subunits/domains alternately take the lead position (SF3-6), or whether one subunit/domain always maintains the lead position (SF1-2) [66].

1.4.1. Inchworm mechanism

In the inchworm mechanism, one subunit/domain always maintains the lead position and then alternates with the other subunit for contacts along the nucleic acid (Fig. 1**B**, i). Monomeric helicases in SF1 and SF2 superfamilies translocate by employing an inchworm mechanism [56]. At least two contact points are made with interchanging tight and loose (analogous to the front and hind leg of an inchworm) interactions are required to maintain this mechanism. While one RecA lobe is tightly bound to the nucleic acid, the other is loosely bound. The loose RecA lobe at the front will dissociate and translocate to bind to the DNA tightly at the forward position. After the loose position moves ahead, the original tight site at the back transitions to a loose conformation and moves forward to regain close proximity with the forward site [67]. Separation of the duplex takes places through at a stable 'pin' or a 'wedge' structure that acts as physical barrier [68]. The tight coupling of the two contact points with the domain rotations results in unidirectional translocation. The direction can be reversed if the two helicase contact sites switch their tight and loose grips with the DNA in coordination with their movement. The crystal structures of PcrA and RecQ DNA helicases complexed with a DNA substrate suggest an inchworm mechanism for translocation [33,69].

Modifications of the inchworm mechanism can include additional subunits binding to the 'trailing face' forming a dimer or linear oligomeric 'marching' complex that promotes stability, prevents slippage, and forces unidirectional translocation utilizing a functional cooperativity mechanism (Fig. 1**B**, ii) [70]. Dda and NS3 appear to utilize this marching mechanism whereby increasing the length of ssDNA and allowing multiple subunits to binding increases unwinding [71,72]. SF1 helicases such as UvrD [73], Rep [74], PcrA [75], and Pif1 [76] can dimerize to increase or activate unwinding, however, other accessory proteins can also fulfill this role [77,78]. In those cases, rotation of the 2B domain on the 'leading face' appears to be influential as a switch-like regulator of unwinding activity [8,79,80]. The 'rolling dimer' model (Fig. 1**B**, iii) was originally proposed for Rep [81,82] based on affinity for both ss and dsDNA and the need for at least a dimer to activate unwinding [83], however, there is now more evidence for the inchworm and 2B regulator model instead. Finally, the heterotrimeric RecBCD helicase nuclease is organized as a bipolar motor (Fig. 1**B**, iv), where RecB translocates 3′-5′ and RecD translocates 5′-3′ effectively splaying the duplex through a pin domain in RecC [13].

1.4.2. Hand-over hand mechanism

In a hand-over hand mechanism, each of the six subunits in hexameric helicases alternately take the lead position as they translocate, akin to a circular staircase (Fig. 1**C**). This mechanism has been observed in various hexameric helicases including E1 [43], gp4 [46], DnaB [84], Rho [48], archaeal MCM [85], and *Drosophila* CMG [86]. Each subunit of the hexameric helicase contain a DNA binding loop aligned with the spiral DNA backbone that maintains a helical conformation even with the single strand. Binding of NTP stabilizes the subunit interface as well as the tight binding to DNA backbone. Once NTP is hydrolyzed and Pi (or NDP + Pi) product is released, both the subunit interface and DNA binding becomes unstable and loose. The subunit with the first NTP hydrolysis, is released from its neighboring subunit and DNA to translocate forward and regain tight binding to DNA. This subunit will then form a new subunit interface to bind ATP. Similarly, each of the remaining five subunits will undergo sequential ATP hydrolysis resulting in subunits successively translocating from one end of the spiral to the other. This translocation mechanism mimics a hand-over-hand movement with each subunit alternatively taking the lead position as they move forward [46,56].

1.5. Unwinding

The process by which the duplex is separated into two strands at the ss-ds junction is known as unwinding. Helicases utilize the energy from NTP hydrolysis to translocate along ssDNA (or ssRNA) and unwind long stretches of the duplex [67]. Translocation of helicases on the oligonucleotide can occur using the mechanisms mentioned above. In general, depending on its mechanism for coupling translocation to unwinding (base-pair separation), there are two models with which enzyme-catalyzed DNA unwinding can be achieved: passive or active.

1.5.1. Passive vs. active unwinding

In an active unwinding model, the helicase directly destabilizes dsDNA by breaking the hydrogen bonds between the DNA base pairs to promote active separation of duplex DNA coupled with ATP hydrolysis. Conversely, in a passive unwinding model, the helicase traps and stabilizes transient single stranded intermediates when thermal fraying partially open dsDNA (internal melting at the duplex end) [83,87]. The major difference between the two unwinding mechanisms is that passive unwinding requires helicase binding only to ssDNA, but active unwinding binds both ss and duplex DNA concurrently to facilitate unwinding [88,89]. For a given helicase, passive unwinding occurs slower than its translocation rate on DNA because the stability of the duplex slows progression, whereas active unwinding can occur as fast as translocation rate on DNA as NTPase activity is linked to destabilization of the duplex [87]. The ratio between the translocation rate to the rate of dsDNA unwinding is a measure to distinguish between the two mechanisms. If this ratio is between 0.25 and 1, the helicase can be considered active. Most helicases have a ratio in between these numbers. Direct evidence for an active unwinding mechanism for Rep, PcrA, RecQ, and Dda DNA helicases has been presented [4,81,89,90].

Passive unwinding mechanism can be utilized for helicases that can translocate and occupy one base at a time at the ss-ds junction. The likelihood of several base-pair opening due to thermal fluctuations is relatively low. Therefore, helicases which occupy several base pairs require an active mechanism to separate DNA [67]. For an instance, while ring-shaped hexameric helicases by themselves can actively unwind dsDNA without the aid of accessory proteins, its rate is relatively slow. The energy from NTP hydrolysis is enough to translocate on ssDNA, but not enough to stably separate the base pairs. The unwinding rate can be rapidly increased when the helicase is coupled to a replicative DNA polymerase that backstops the helicase and provides additional energy from dNTP hydrolysis to aid forward progression [91,92]. This coupled unwinding rate is then on par with the helicase ssDNA translocation rate suggesting an active unwinding mechanism for the complex [93,94]. Polymerases also prevent reannealing of the unwound DNA by immediately using the unwound ssDNA as templates to synthesize new duplex DNA. Interestingly, recent single molecule studies suggest a mechanism, where passive unwinding performed by *E. coli* DnaB helicase is driven primarily by the energy provided by the leading strand DNA polymerase incorporating deoxyribonucleotides [95]. Alternatively, the single-stranded DNA binding protein (SSB) can occupy the ss-ds junctions opened up due to thermal fraying and continue aid in the passive unwinding of the duplex DNA and promote DNA unwinding [96,97].

1.5.2. Steric exclusion models

Numerous replicative and non-replicative helicases are shown to unwind dsDNA by actively translocating along one strand while the

other being physically excluded. This process is referred to generally as Steric Exclusion (SE) with an external DNA winding point acting as a wedge [67]. Several ring-shaped helicases including DnaB, MCM, T7 gp4 as well as non ring-shaped helicases such as NPH-II and Dda have been proposed to unwind by this general mechanism [98–100]. As described above, the helicase will have a tight grip on the encircled strand while translocating with a specific polarity. Depending on the exact role of the excluded strand during unwinding, several modifications to the SE model have also been proposed (Fig. 1**C**) [61].

In the classic steric exclusion (SE) model, the excluded strand does not have any interaction or contact with the helicase (Fig. 1**C**, i). While this model proposes a way to prevent immediate reannealing of the unwound DNA strands, it lacks any functional or regulatory role for the excluded strand. The mechanism for SE model became evident when biochemical studies on model systems disclosed helicases' ability to bypass a bulky adduct on the excluded strand, but not on the encircled strand [101].

The steric exclusion and wrapping (SEW) model suggested a functional or regulatory role for the excluded strand (Fig. 1**C**, ii). In this evolved model of SE, the excluded strand interacts with the external surface residues of the helicase and partially wraps around it. The proposed function for SEW include helicase stability, prevention of backward sliding, and regulation of enzymatic activity such as unwinding. This model has been suggested for archaeal MCM helicase [102] and *E. coli* DnaB helicase [103].

In the modified steric exclusion (MSE) model, both DNA strands initially enter the helicase pore on the leading face (Fig. 1**C**, iii). Then the non-translocating strand is separated internally and extruded back from the same channel, while the encircled strand continues through the central channel. The key difference here from SE or SEW is that the wedge for unwinding occurs internally within the hexamer instead of externally. This type of MSE has been proposed primarily for the eukaryotic CMG helicase [104].

The side channel extrusion (SCE) model describes a process where duplex DNA enters the helicase central channel, separation of the strands (*i.e.,* wedge) occurs internally, and then the non-translocating strand is extruded back out from a side channel within the middle of the helicase subunit. SCE has been proposed for SV40 L-Tag [105]. There is evidence suggesting a SE [44] or SCE [106] mechanism for the E1 helicase, however a recent cryo-EM structure of E1 bound to a fork DNA substrate clearly shows the 5′ excluded strand interacting with one of the six dsDNA binding domain (OBD) of the hexamer to facilitate separation by SE or SEW [107].

2. Determining static binding orientations

Our understanding of the mechanisms that govern the translocation/unwinding processes by replicative helicases has been enormously enriched by a combination of biochemical, biophysical, and structural studies. In this section, we will discuss and compare different experimentation methods based on their potential to study static binding orientations of diverse helicases.

Biochemical methods

There are numerous methods that have been developed both *in vivo* and *in vitro* to monitor protein-DNA complexes. Although there are others including filter binding assays, isothermal titration calorimetry [18], analytical ultracentrifugation, and presteady-state approaches to measure k_{on} and k_{off} directly, some of the most prominently utilized techniques used *in vitro* to identify protein-DNA interactions and specificities are electrophoretic mobility shift assay (EMSA), fluorescence anisotropy (FA), and measuring DNA unwinding directly **(**Fig. 3**A-C)**.

2.0.1. Electrophoretic mobility shift assay (EMSA)

EMSA is a routinely used rapid and sensitive method that permits visualizing the interaction between a protein and DNA substrate. Reactions containing a constant amount of end-labelled DNA (either ^{32}P or fluorescent) with increasing concentrations of the protein of interest are incubated together to establish an equilibrium. The products can be resolved on a native polyacrylamide gel matrix with high resolution to separate the free DNA from the bound protein-DNA complexes **(**Fig. 3**A)**. EMSA can be used to determine the fraction of bound complex versus free nucleic acid, and using a variety of equations can calculate the apparent equilibrium dissociation constants or indicate cooperativity [108]. The strengths of EMSA are its ability to determine the presence of different protein oligomeric conformations, sensitivity, sequence or DNA structure specificities, and binding site distribution on DNA. However, it cannot be used to validate the orientation of a protein with respect to the polarity of the bound DNA.

2.0.2. Fluorescence anisotropy (FA)

FA is based on the change in fluorescence polarization upon protein binding to a fluorescently labeled nucleic acid **(**Fig. 3**B)** [109]. Similar to EMSA, anisotropy can also help determine the binding affinity, specificity, and any cooperativity through fitting the change in anisotropy to a variety of equations. However, FA does not provide positional information of the protein on DNA, nor does it actually reveal multiply bound states or conformations which can confuse the analysis. Both EMSA and FA are equilibrium binding techniques, and it is important to make sure that a sufficient equilibrium is established for the experiment [110]. There is also a host of solution, substrate, concentration, and environmental conditions that can significantly affect measured binding affinities. Therefore, it is important to fully test and understand (with appropriate controls) a specific binding experiment to reduce potential variability.

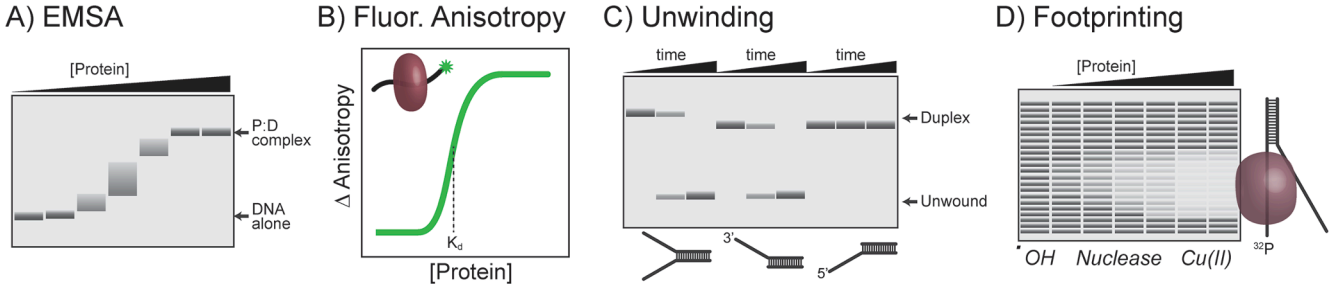

Fig. 3. Static binding techniques to determine substrate affinity and specificity. A) Electrophoretic mobility shift assay (EMSA) shows then decrease in mobility through a gel upon protein binding to a labelled oligonucleotide. B) Fluorescence anisotropy (FA) shows an increase in polarization and resulting anisotropy upon titration of a protein into a fluorescently labelled oligonucleotide. A low concentration of the labeled DNA can be titrated against an increasing concentration of the protein to obtain the affinity (K_d) between the DNA and protein complex [172]. C) Traditional unwinding experiments can define substrate specificity for helicases resolved on native gels. D) Chemical or enzymatic footprinting can identify site specific binding positioning for proteins based on a protection pattern after digestion. All these images are cartoon representations of experiments and not real data.

2.0.3. Unwinding polarity specificity

Unwinding experiments measure the rate of NTP- dependent helicase enzyme- catalyzed dsDNA (or RNA) separation over time or at increasing protein concentrations (**Fig. 3C**). Based on its physiological function, helicases from different organisms can unwind a wide variety of duplex substrates including fork substrates, or substrates with 3′ or 5′ arms. The products can be separated on a native polyacrylamide gel to separate the duplex from the unwound ssDNA substrate. Fig. 3**C** is a representation of a helicase that translocates in the 3′-5′ direction to unwind duplex DNA and can do so for fork or 3′ single arm substrates. Even though, unwinding experiments can detect the translocation polarity of a helicase, it cannot determine the orientation of the helicase while actively translocating.

2.0.4. Traditional footprinting

Traditional footprinting methods have been widely employed to study DNA (or RNA)-protein complexes, specially to determine the binding site size, specificity, and positioning of a protein bound to an oligonucleotide. When a protein is bound to a specific sequence, the protein bound portion is protected from attack by chemical reagents or endonucleases, while the unbound portion of the DNA molecule is free to react [111,112]. Footprinting reagents can be specific for ssDNA (*i.e.* $KMnO_4$ [113,114], S1 nuclease [115], mung bean nuclease [102]) or more nonspecifically for ss or dsDNA (DNaseI [116], hydroxy radical [111,117] or micrococcal nuclease [118]). In this way, it is possible to identify helicase protected regions of ss or dsDNA or hypersensitive sites that are distorted upon binding, activation, or unwinding. Cleavage products are separated on a denaturing polyacrylamide gel to identify protein-binding sites on the nucleic acid from ^{32}P or fluorescent end labelling and protection from digestion. The cleavage products will be visualized as a ladder of bands. The protected protein binding sites are revealed by the diminished bands present in the gel (Fig. 3**D, light grey bands**). Similar to the biochemical methods discussed above, traditional footprinting methods lack the ability to determine the bound or translocation orientation of the helicase bound to the DNA, but it can be used to monitor helicase positioning on a variety of substrates.

2.0.5. Site-specific footprinting

Biochemical methods that employ site-specific footprinting can be utilized to determine the static binding orientation of a protein bound to a specific sequence. Few examples of chemical reagents that can be used for site specific footprinting are 4-azidophenacyl bromide (APB), S-(2-pyridylthio)cysteaminyl-EDTA, and 1-(p-Bromoacetamidobenzyl) ethylenediamine N, N,N (Fe-BABE). Several studies have been conducted with these crosslinking reagents to study the static binding orientations of proteins on DNA [119–121]. We have previously studied the static binding orientation of *Saccharolobus solfataricus* MCM helicase on DNA using both APB and Fe-BABE [49,122]. Both these crosslinking agents contain a bromide functional group that reacts with a reduced thiol (*e.g.*

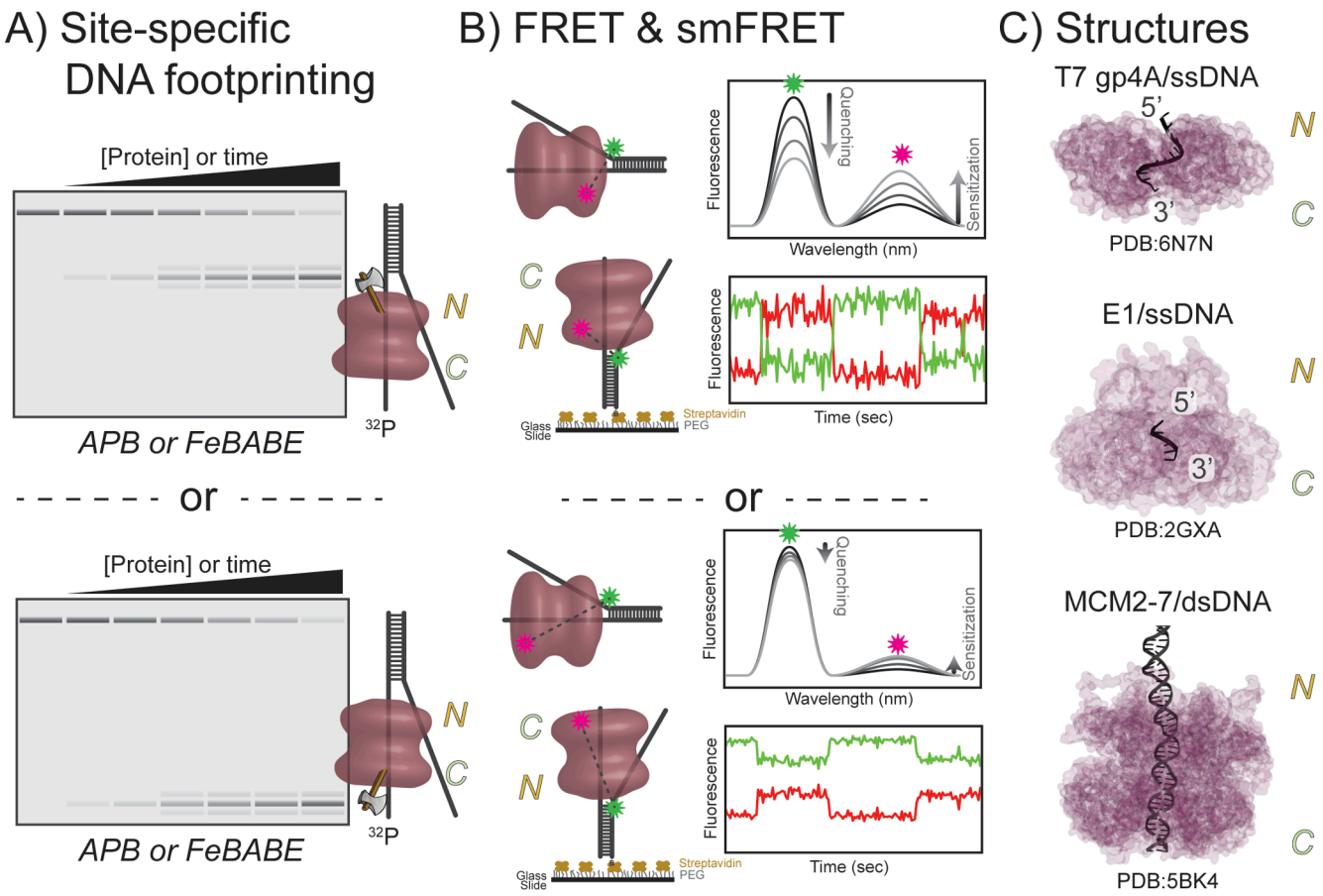

Fig. 4. Determining static binding orientations of helicases. A) Site-specific footprinting can be used to isolate a nuclease reaction to a specific region of a protein through conjugation to identify N-first binding [49]. The axe denotes the position of the site-specific DNA cleavage agent attached at either the N or C-terminal domain. B) FRET and smFRET can utilize spectral signals from an appropriated placed fluorescent donor dye at the fork junction and acceptor dyes at either the NTD (top panel) or the CTD (bottom panel) to monitor relative distances of bound species to correlate with N-first [49]. All these images are cartoon representations of actual experiments and not real data. C) Helicase-nucleic acid structures can provide high resolution snapshots of static binding orientations [43,46,140], where the NTD (N) and the CTD (C) are indicated relative to the 3′ and 5′ ends of the encircled strand.

solvent accessible cysteine amino acid) at either the NTD or CTD faces (Fig. 4**A)** by S- alkylation to form stable thioester products. After incubating these functionalized protein products with labeled DNA, cleavage can be induced by either UV/NaOH (APB) or hydrogen peroxide and ascorbic acid (Fe-BABE) at nucleotides in the closest proximity and within a limited radius of the cleavage agent. The resulting DNA cleavage products can be separated on native or denaturing acrylamide gels to analyze lengths and cutting patterns. As an example, for a protein of interest that loads onto a fork DNA with the NTD at the duplex, crosslinking with a cysteine within the NTD will result in cleavage of the substrate in the middles (Fig. 4**A, upper panel)**, whereas crosslinking with a cysteine at the CTD will provide very short DNA fragments (Fig. 4**A, lower panel)**. The ^{32}P or fluorescent labeling can occur at either ends and provide different cutting patterns for confirmation. Therefore, site-specific footprinting can be utilized to determine the static binding orientation of a protein of interest on DNA; thus providing a major advantage from the techniques described above. However, this method will not directly confirm the translocation orientation of a protein during active unwinding and just reports on static states that may include multiple orientations.

FRET and smFRET

Steady-state fluorescence resonance energy transfer [123] or single molecule FRET (smFRET) can also be used to monitor the relative binding positions between two donor and acceptor fluorescence dyes (Fig. 4**B**). FRET relies on quantifying the efficiencies of the overlapping spectra of two interacting dyes and has been applied to a variety of biological systems, acting as a molecular ruler [124,125]. When FRET is applied by labelling a helicase and an oligonucleotide at specific limiting sites, the relative bound orientations can be determined [126]. FRET and its more recent cousin, protein induced fluorescence enhancement (PIFE) [127,128], are also commonly used to quantify binding affinities for protein–protein or protein-DNA species [129], complementing EMSA and FA described above. smFRET has also been effectively utilized to examine the dynamics of helicase/oligonucleotide complexes for a variety of systems [130], taking advantage of single-pair or multicolor labeling [131]. The advantage of smFRET is that it generally includes a time dimension for individual molecules, allowing the analysis of distributions and the dynamics of binding for a population. This time domain can be important in better confirming translocation orientation; however, the characterization is not absolute.

For example, we had previously combined analyses of MCM binding to various DNA substrates using steady-state FRET [132] and smFRET [133] and incorrectly inferred a particular translocation orientation based on static binding. The static equilibria data indicated that the majority of MCM hexamer species were bound with the CTD at the duplex fork junction. This result may be more representative for the initial origin bound and loaded state of the double hexamer, where the CTD would be at the duplex side of an activated open state and not that of the active unwinding hexamer. Later, we were able to characterize the binding population distributions of the hexamer on various substrates and utilize single-turnover kinetics and presteady-state FRET to determine an N-first orientation of the active translocating hexamer [49]. The lesson is that static (or population) binding orientations provide information on equilibria binding properties but do not confirm translocation orientations for active species.

2.1. Structures, X-ray and EM

Several prominent publications examining static structural features of various helicase on DNA using X-ray crystallography [13,27,29,33,42,43,46,69,85,134,135] and cryo- EM [50,136–143] have been valuable for inferring the static binding orientation of helicases/translocases on DNA and providing insights into the translocation and/or unwinding mechanisms (Fig. 4**C**). Once again, these structures are static equilibrium bound states, and although there are various crystal lattice forms and EM sub-classes that can represent probable dynamic states, they remain snapshots. Helicase structures that include oligonucleotides are particularly influential as combined with validating biochemistry on the substrate preference and measure polarities, they can be used to predict the translocation orientation and the leading face of the helicase (Table 1). Structures of helicases in complexed with oligonucleotide and/or other interacting proteins continue to be highly valuable in assigning relative orientation of these complexes in more accurately describing directionality as evident by structures of the T7 replisome [46], eukaryotic CMG-Polε [136,143], and papilloma virus E1 helicase [107].

3. Determining active translocation orientations

Of course, any true determination of translocation orientation will require a time element to monitor progress in direct relation to the DNA substrate. As outlined above, determination of static binding orientations (Fig. 2**)** can provide strong insights into mechanism, however, only when monitoring dynamic processes can the translocation orientation be absolutely determined.

Building on experiments and concepts described above, many of those techniques can be adapted to include a time dimension to understand structural processes of translocation through kinetic assays. For this to be conclusive, information on both the structure and relative orientation as related to the nucleic acid polymer needs to be monitored upon translocation initiation. Fortunately, many helicases and translocases are initiated with either addition of Mg^{2+} or ATP, other energy sources, or firing factors making this a convenient time zero. If these cofactors can easily be introduced into the reaction in a continuous or discontinuous but time dependent manner, then it is possible to watch translocation orientation directly using a variety of methods.

3.1. Time resolved DNA footprinting

Although traditional footprinting (Fig. 3**D**) or site specific footprinting (Fig. 4**A**) are static experiments, induction of ATP can activate translocation and the resulting DNA cleavage can be monitored as a function of time to determine translocation orientation (Fig. 5**A**). One good example is following nucleosome remodeling or repositioning by SF2 family Snf2-type ATPase motors [144,145]. These motors share common structures that include two RecA-type ATPase domains or lobes that cradle each of the DNA strands. For translocation, the two lobes alternate between a closed ATP bound state and a more open ADP or nucleotide free state that ratchets the remodeler along in 1–2 base steps. Moving in the 3′-5′ direction, lobe 2 is on the front edge, while lobe 1 is behind. After ATP hydrolysis, lobe 2 in. forward to an open state, allowing for exchange of ADP with ATP stimulating a closed state where lobe 2 moves forward to recreate the ATPase active site.

Translocation direction of the chromodomain helicase DNA-binding protein 1 (Chd1) was confirmed by using the 601 Widom positioning sequence, the structure and orientation of the nucleosome, and the static structure of Chd1 bound to a nucleosome [146]. Upon addition of Chd1, the nucleosome is pushed directionally along the sequence as detected by site-specific APB attachment to the nucleosome and resulting change in footprinting, indirectly confirming the translocation orientation of Chd1. This nucleosome movement can be explained through changes in DNA twist or defects enforced by Chd1 that result in 1 bp movements, resulting from ratcheting of DNA directed by the ATP hydrolysis cycle and the lobe movements [21,145,147]. Similar directional positioning of nucleosomes by stepping for related Snf2 remodelers have been observed for SWI/SNF [148], ISWI [149], and INO80 [141] allowing for absolute determination of an overall conserved active translocation orientation of these bilobed enzymes.

3.2. Presteady-state FRET

Presteady-state methods, including stopped-flow and rapid quench, are outstanding methods to introduce or mix reaction components with

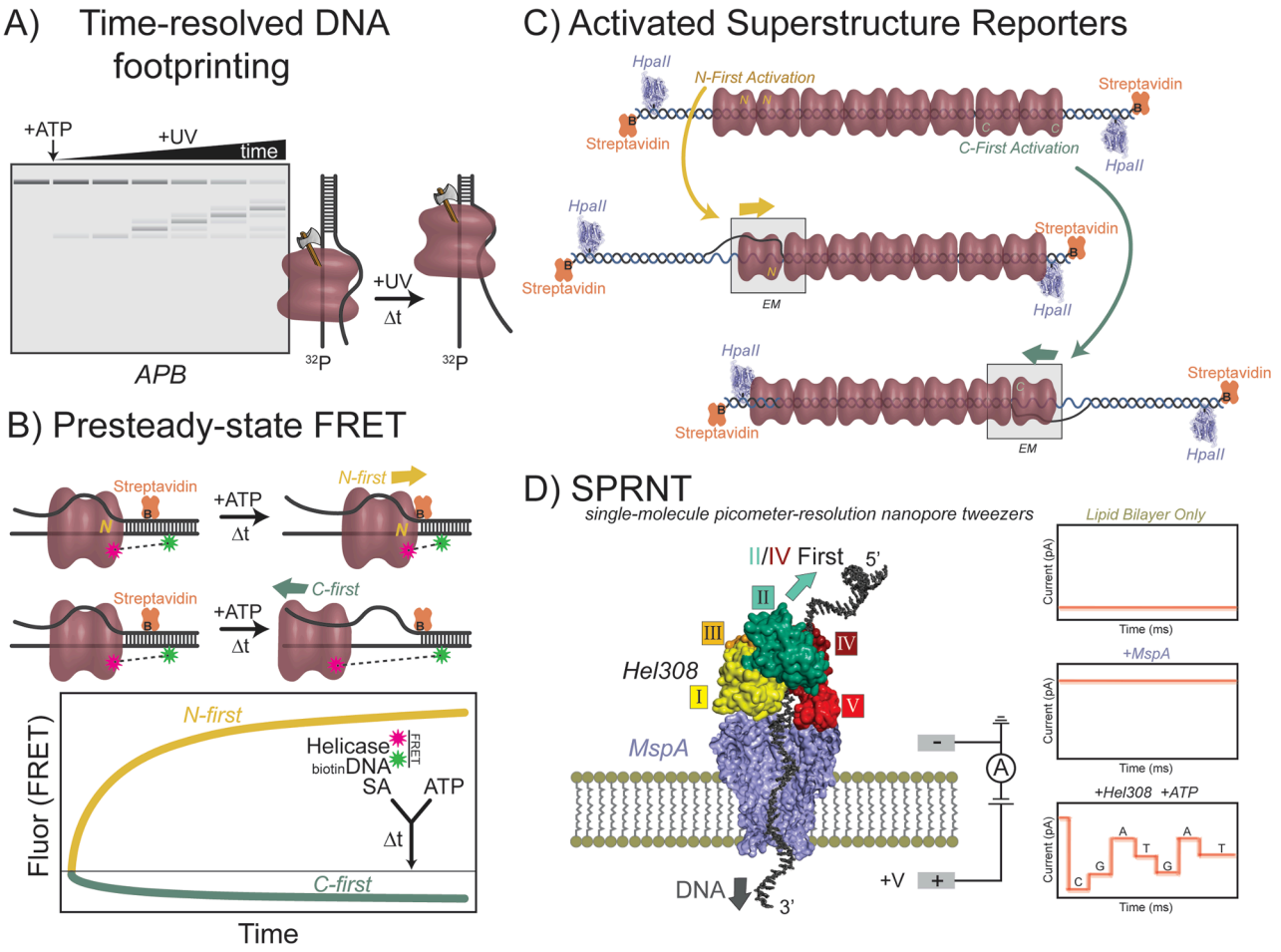

Fig. 5. Methods for determining active translocation orientations of helicases. A) Site-specific footprinting can be combined with an enzyme initiation event and/or nuclease activation to monitor translocation progress. B) Presteady-state FRET assays [49] can be designed to detect translocation directly upon initiation with ATP and enriched at a stalled downstream state. C) Activated cryo-EM superstructure reporters [136] can be utilized to monitor changes in conformations of reporter subunits coupled with structural information on the active subunit to determine translocation direction. D) Single-molecule picometer-resolution nanopore tweezers (SPRNT) can translocate DNA through a sequencing pore [171] to indicate absolute translocation orientation of Hel308. All these images are cartoon representations of actual or possible experiments and not real data.

millisecond (or better) resolutions. They have been used repeatedly to understand and characterize kinetics for a variety of helicases [150–154]. However, to add a structural dimension to translocation, proteins or DNA or both need to be labelled with fluorophores at defined sites to detect relative changes in distances that can be correlated with known structures. Just measuring the kinetics of unwinding/translocation without structural context will be misleading.

Previously, we developed a presteady-state assay that could directly monitor unwinding orientation of the first few base pairs of a DNA duplex before being stalled by a physical biotin/streptavidin block (Fig. 5**B**) [49]. The design is different from other presteady-state assays that are used to detect unwinding/translocation polarity or speed [152,154]. With those assays, it is impossible to detect translocation orientation as fluorescence labels on the leading face of the helicase will have very similar kinetics to those on the trailing face. Instead, we designed an assay that will result in an increase in FRET with a fluorophore on the leading face and either no change or a decrease in FRET with a fluorophore on the trailing face. The key here is utilizing Forster distance limitations in concert with a specific stalled state. For *Sso*MCM, fluorescence labelling on the N-terminal tier resulted in an increase in fluorescence, while labeling at the C-terminal tier resulted in a decrease, establishing that unwinding proceeds N-first with 3′-5′ polarity. In this case, it did not matter that the helicase is a hexamer as all of the N-terminal domains are arranged symmetrically to one face.

This method can be applied for other helicase/translocations; however, there are some limitations. First, appropriate sites on the helicase for fluorescent labelling need to be designed utilizing available proteins structures, either through cysteine mutations or other more advanced biorthogonal methods. Second, the DNA substrate needs to have a fluorescence label incorporated to detect advancing FRET. Third, unwinding needs to be stalled such that the leading face would provide the greatest FRET signal while simultaneously limiting any FRET when labeled at the trailing face. Stalling of the helicase becomes important because labeling on the trailing face would also provide a transient increase in FRET that may be misinterpreted.

3.3. *Single-molecule FRET (smFRET)*

Generally, smFRET already includes a time dimension and addition of ATP or other firing factors that can initiate enzyme action. Similarly, PIFE can detect kinetics or dynamics with only one fluorophore [155,156]. Although both smFRET and PIFE can detect movement and dynamics, structural information is required to determine a relative orientation during unwinding or translocation. When structures are utilized in smFRET design and analysis, translocation can be adequately inferred as for PcrA (3′-5′, 2A-First) [6]; UvrD (3′-5′, 2B-First) [8], Rep (3′-5′, 2B-First) [157]; Pif1 (5′-3′, 1A/2B-first) [158]; DHX36 (3′-5′, RecA2-first) [17]; WRN (3′-5′, C-first) [123]; T7 gp4 (5′-3′, C-First)

[159]; E1 (3′-5′, N-First) [44]; among others (Table 1). smFRET experiments with Chd1 were able to reveal more details on the steps and unstable intermediates involved with nucleosome remodeling and showed that bidirectional remodeling occurs with ATP and can shift nucleosomes [8] back and forth [160]. There is a big push to integrate smFRET with structural modeling and molecular dynamics for a more accurate picture of structure–function relationships of enzyme complexes including helicases and translocases [161].

Other single molecule methods, including magnetic [162] or optical tweezers/traps [163,164] have been utilized successfully to examine various kinetic properties for a number of helicases and replisome complexes, but generally do not have the resolution or structural integration to determine translocation orientation. However, combining optical trapping with fluorescence imaging [139,165] has the potential to improve resolution to a point where relative orientation of enzymes can be monitored in addition to translocation or unwinding.

3.4. Electron microscopy reporters

Another creative way to detect translocation orientation is using indirect or direct protein markers and applying structural biology methods. Having the structure of helicase complexes really helps with the prediction of translocation orientation, however generally, this is still a static snapshot. The incorporation of streptavidin or methyltransferase protein blocks to unwinding can provide binding context to yeast CMG as visualized by cryo-EM [50,86,104] as well as inform on the unwinding mechanism (Fig. 1B, *MSE*). However, when helicase translocation or unwinding can be activated through addition of ATP, other cofactors, or firing factors, then the resulting assemblies, loading, and translocation can be monitored as a function of time [166]. If translocation or unwinding can be related to or directly impact positional reporters, then the process can be monitored using activated superstructures (Fig. 5**C**). This was recently performed with several yeast CMG double hexamers loaded onto DNA. Covalent protein roadblocks were incorporated into the DNA substrate to prevent the 'pushing off' of CMG hexamers after activation with kinases and protein firing factors. Only a subset of CMG hexamers is activated that pushed inactive CMGs along the DNA template directionally. This resulted in the appearance of CMG 'train cars', where the active CMG 'engine' will be in the middle of the DNA complex. Zooming in on the CMG engine can identify the orientation and determine which domain is on the leading face. In this case with CMG, it was determined that the N-terminal domain is the leading face [136], consistent with other reports of CMG helicase [50,86] and later results from archaeal MCM [49,85].

3.5. Time resolved structural biology methods

Based on several influential publications following enzyme action of DNA polymerases within a crystal and subsequent time resolved x-ray crystallography (tr-Xray) of their transient structures [167,168], it may also be possible to similarly study helicase or translocase movement along a nucleic acid template. However, the crystal lattice will likely limit large-scale conformational changes that occur and could be a major barrier for observing helicase translocation *in crystallo*. The revelation of the minimal T7 replisome structure by cryo-EM [46] provides a firmer context for DNA unwinding by the helicase by utilizing relative positioning of other replisome proteins including the polymerase and primase. Although still static pictures, the three class averages showed a movement of one of the six helicase subunits around the cracked ring structure to suggest a hand-over-hand translocation mechanism. One caveat in this study is that although subunit movement is presented as stepping movements from one subunit to the next, a time dimension is not present to confirm directionality of movement. It would be extremely interesting and highly valuable if these domain movements could be detected in real time. However, these helicase domain motions are quite a bit larger than those detected for nucleotide incorporation and translocation in DNA polymerases and may be impossible for tr-Xray and difficult to image rapidly in cryo-EM. That said, advances in cryo-EM are occurring swiftly [169]. Time resolved cryo-EM [170] is showing promise and may be amenable to rapid mixing and freezing of helicase/translocase complexes after addition of various firing factors.

3.6. Nanopore contexts

When visualizing translocation orientation, it is often considered from the standpoint of the enzyme instead of the substrate. However, translocation of nucleic acid polymers through an immobilized enzyme can also provide a direct measure of orientation. This is becoming more prevalent with advancements in nanopore sequencing of DNA. A good example involves the attachment of the helicase, *i.e.* Hel308, to a protein nanopore, MspA, embedded within a membrane (Fig. 5**D**) [40,171]. Hel308 can then actively translocate (or unwind) on a ssDNA substrate through the nanopore for electrochemical detection of DNA bases for sequencing in a method termed single-molecule picometer-resolution nanopore tweezers, SPRNT. Hel308 is a SF2 helicase that translocates 3′-5′ and is organized as a five-domain enzyme [38,39]. Although these crystal structures contained a 3′ overhang substrate that placed RecA domain 2 and rachet domain 4 on the leading face of the enzyme and adjacent to the duplex, this was only highly suggestive of the unwinding mechanism. It is not until it was possible to monitor kinetic processes in context with structural features to be certain of the translocation orientation.

They key here is that ssDNA is fed through MspA in the 3′ to 5′ direction and Hel308 interacts with and is immobilized by MspA through the other RecA domain 1 and helix-loop-helix domain 5. Therefore, the actual translocation orientation of Hel308 along ssDNA can be confirmed with domain 2/4 on the leading face (Fig. 5**D**). Subsequent sequencing of ssDNA is accomplished by detecting the absolute changes in current that correspond to specific DNA bases. The result is a fast, specific, and inexpensive third generation prototype for DNA sequencing. It is likely that other helicase or translocases can be engineered in this nanopore fashion to resolve mechanisms of translocation, step sizes, orientation, unwinding as well as improve or expand DNA sequencing methods.

4. Conclusions

Although traditional biochemistry and structural biology methods continue to be the dominant methods for helicase characterizations, advances in time-resolved methods can provide greater insight into a more complete mechanism of translocation and unwinding. There will continue to be an integration of chemical, biochemical, structural biology, and kinetic methods to better characterize nucleic acid translocation. As more interactions are discovered and then characterized, their positioning can be influential in understanding the translocation orientation of the entire complex. Substrate specificities, binding affinities, and translocation polarities are useful in biochemically characterizing the diverse nature of helicase/translocases. Structures of enzymes bound to nucleic acid substrates or with interacting subunits within unwindosome complexes provide a higher resolution on structure function relationships. Incorporating kinetics and motion into structural biology of complexes will provide the greatest validation of helicase/translocation processes both *in vitro* and ultimately *in vivo* and unequivocally assign active translocation orientations. Helicases and translocases are some of the best characterized motor proteins, and they are intriguing therapeutic drug targets for a variety of diseases including cancer, aging, fertility, and neurodegenerative diseases. Having a better more in depth understanding of the enzymatic abilities, structure–function relationships, and translocation orientations will undoubtedly be valuable in targeting these enzymes for future therapies.

5. Funding sources

This work is funded by the NSF-MCB (1613534 & 2105167 to M.A.T.) and the NIH R15 (GM13791 to M.A.T.).

Declaration of Competing Interest

The authors declare that they have no known competing financial interests or personal relationships that could have appeared to influence the work reported in this paper.

References

[1] M.R. Singleton, M.S. Dillingham, D.B. Wigley, Structure and mechanism of helicases and nucleic acid translocases, Annu. Rev. Biochem. 76 (1) (2007) 23–50.
[2] A.E. Gorbalenya, E.V. Koonin, Helicases: Amino acid sequence comparisons and structure-function relationships, Curr. Opin. Struc. Biol. 3 (3) (1993) 419–429.
[3] M.E. Fairman-Williams, U.P. Guenther, E. Jankowsky, SF1 and SF2 helicases: Family matters, Curr. Opin. Struc. Biol. 20 (3) (2010) 313–324.
[4] K.D. Raney, A.K. Byrd, S. Aarattuthodiyil, Structure and mechanisms of SF1 DNA helicases, Adv. Exp. Med. Biol. 973 (2013) E1.
[5] A.K. Byrd, K.D. Raney, Superfamily 2 helicases, Front. Biosci. 17 (2012) 2070–2088.
[6] J. Park, S. Myong, A. Niedziela-Majka, K.S. Lee, J. Yu, T.M. Lohman, T. Ha, PcrA helicase dismantles RecA filaments by reeling in DNA in uniform steps, Cell 142 (4) (2010) 544–555.
[7] M. Stelter, S. Acajjaoui, S. McSweeney, J. Timmins, S. Korolev, Structural and mechanistic insight into DNA unwinding by *Deinococcus radiodurans* UvrD, PLoS ONE 8 (10) (2013) e77364.
[8] B. Nguyen, Y. Ordabayev, J.E. Sokoloski, E. Weiland, T.M. Lohman, Large domain movements upon UvrD dimerization and helicase activation, Proc. Natl. Acad. Sci. USA 114 (46) (2017) 12178–12183.
[9] J.G. Bruning, J.A.L. Howard, K.K. Myka, M.S. Dillingham, P. McGlynn, The 2B subdomain of Rep helicase links translocation along DNA with protein displacement, Nucl. Acids Res. 46 (17) (2018) 8917–8925.
[10] X. He, A. Byrd, M.-K. Yun, C. Pemble, D. Harrison, L. Yeruva, C. Dahl, K. Kreuzer, K. Raney, S. White, The T4 phage SF1B helicase Dda Is structurally optimized to perform DNA strand separation, Structure 20 (7) (2012) 1189–1200.
[11] N. Su, A.K. Byrd, S.R. Bharath, O. Yang, Y.u. Jia, X. Tang, T. Ha, K.D. Raney, H. Song, Structural basis for DNA unwinding at forked dsDNA by two coordinating Pif1 helicases, Nat. Commun. 10 (1) (2019), https://doi.org/10.1038/s41467-019-13414-9.
[12] F. Xie, C.G. Wu, E. Weiland, T.M. Lohman, Asymmetric regulation of bipolar single-stranded DNA translocation by the two motors within *Escherichia coli* RecBCD helicase, J. Biol. Chem. 288 (2) (2013) 1055–1064.
[13] M.R. Singleton, M.S. Dillingham, M. Gaudier, S.C. Kowalczykowski, D.B. Wigley, Crystal structure of RecBCD enzyme reveals a machine for processing DNA breaks, Nature 432 (7014) (2004) 187–193.
[14] K. Saikrishnan, S.P. Griffiths, N. Cook, R. Court, D.B. Wigley, DNA binding to RecD: Role of the 1B domain in SF1B helicase activity, EMBO J. 27 (16) (2008) 2222–2229.
[15] S. Raj, D. Bagchi, J.V. Orero, J. Banroques, N.K. Tanner, V. Croquette, Mechanistic characterization of the DEAD-box RNA helicase Ded1 from yeast as revealed by a novel technique using single-molecule magnetic tweezers, Nucleic Acids Res. 47 (7) (2019) 3699–3710.
[16] Q. Yang, E. Jankowsky, The DEAD-box protein Ded1 unwinds RNA duplexes by a mode distinct from translocating helicases, Nat. Struct. Mol. Biol. 13 (11) (2006) 981–986.
[17] M.C. Chen, R. Tippana, N.A. Demeshkina, P. Murat, S. Balasubramanian, S. Myong, A.R. Ferré-D'Amaré, Structural basis of G-quadruplex unfolding by the DEAH/RHA helicase DHX36, Nature 558 (7710) (2018) 465–469.
[18] F. Rozen, I. Edery, K. Meerovitch, T.E. Dever, W.C. Merrick, N. Sonenberg, Bidirectional RNA helicase activity of eucaryotic translation initiation factors 4A and 4F, Mol. Cell Biol. 10 (3) (1990) 1134–1144.
[19] N. Lengert, J. Spies, B. Drossel, Rad54 phosphorylation promotes homologous recombination by balancing Rad54 mobility and DNA binding, Biophys. J. 116 (8) (2019) 1406–1419.
[20] G. Hauk, G.D. Bowman, Structural insights into regulation and action of SWI2/SNF2 ATPases, Curr. Opin. Struc. Biol. 21 (6) (2011) 719–727.
[21] I.M. Nodelman Z. Shen R.F. Levendosky G.D. Bowman Autoinhibitory elements of the Chd1 remodeler block initiation of twist defects by destabilizing the ATPase motor on the nucleosome Proc. Natl. Acad. Sci. U. S. A. 118 4 2021 e2014498118 10.1073/pnas.2014498118.
[22] M.F. White, Structure, function and evolution of the XPD family of iron-sulfur-containing 5 '-> 3 ' DNA helicases, Biochem. Soc. Trans. 37 (2009) 547–551.
[23] D. Constantinescu-Aruxandei, B. Petrovic-Stojanovska, J.C. Penedo, M.F. White, J.H. Naismith, Mechanism of DNA loading by the DNA repair helicase XPD, Nucleic Acids Res. 44 (6) (2016) 2806–2815.
[24] S. Peissert, F. Sauer, D.B. Grabarczyk, C. Braun, G. Sander, A. Poterszman, J.-M. Egly, J. Kuper, C. Kisker, In TFIIH the Arch domain of XPD is mechanistically essential for transcription and DNA repair, Nat. Commun. 11 (1) (2020), https://doi.org/10.1038/s41467-020-15241-9.
[25] L. Fan, J.O. Fuss, Q.J. Cheng, A.S. Arvai, M. Hammel, V.A. Roberts, P.K. Cooper, J.A. Tainer, XPD helicase structures and activities: Insights into the cancer and aging phenotypes from XPD mutations, Cell 133 (5) (2008) 789–800.
[26] Z. Sun, H.Y. Tan, P.R. Bianco, Y.L. Lyubchenko, Remodeling of RecG helicase at the DNA replication fork by SSB protein, Sci. Rep. 5 (1) (2015), https://doi.org/10.1038/srep09625.
[27] M.R. Singleton, S. Scaife, D.B. Wigley, Structural analysis of DNA replication fork reversal by RecG, Cell 107 (1) (2001) 79–89.
[28] T.A. Windgassen, M. Leroux, S.J. Sandler, J.L. Keck, Function of a strand-separation pin element in the PriA DNA replication restart helicase, J. Biol. Chem. 294 (8) (2019) 2801–5614.
[29] T.A. Windgassen, M. Leroux, K.A. Satyshur, S.J. Sandler, J.L. Keck, Structure-specific DNA replication-fork recognition directs helicase and replication restart activities of the PriA helicase, Proc. Natl. Acad. Sci. USA 115 (39) (2018) E9075–E9084.
[30] A. Vindigni, I.D. Hickson, RecQ helicases: multiple structures for multiple functions? HFSP J. 3 (3) (2009) 153–164.
[31] J.A. Newman, A.E. Gavard, S. Lieb, M.C. Ravichandran, K. Hauer, P. Werni, L. Geist, J. Böttcher, J.R. Engen, K. Rumpel, M. Samwer, M. Petronczki, O. Gileadi, Structure of the helicase core of Werner helicase, a key target in microsatellite instability cancers, Life Sci Alliance 4 (1) (2021) e202000795, https://doi.org/10.26508/lsa:202000795.
[32] K. Kitano, S.-Y. Kim, T. Hakoshima, Structural basis for DNA strand separation by the unconventional winged-helix domain of RecQ helicase WRN, Structure 18 (2) (2010) 177–187.
[33] K.A. Manthei, M.C. Hill, J.E. Burke, S.E. Butcher, J.L. Keck, Structural mechanisms of DNA binding and unwinding in bacterial RecQ helicases, Proc. Natl. Acad. Sci. USA 112 (14) (2015) 4292–4297.
[34] T. Saito, D.M. Owen, F. Jiang, J. Marcotrigiano, M. Gale Jr., Innate immunity induced by composition-dependent RIG-I recognition of hepatitis C virus RNA, Nature 454 (7203) (2008) 523–527.
[35] K. Takahasi, M. Yoneyama, T. Nishihori, R. Hirai, H. Kumeta, R. Narita, M. Gale, F. Inagaki, T. Fujita, Nonself RNA-sensing mechanism of RIG-I helicase and activation of antiviral immune responses, Mol. Cell 29 (4) (2008) 428–440.
[36] S. Myong, S. Cui, P.V. Cornish, A. Kirchhofer, M.U. Gack, J.U. Jung, K.-P. Hopfner, T. Ha, Cytosolic viral sensor RIG-I is a 5 '-triphosphate-dependent translocase on double-stranded RNA, Science 323 (5917) (2009) 1070–1074.
[37] S.J. Johnson, R.N. Jackson, Ski2-like RNA helicase structures: common themes and complex assemblies, RNA Biol 10 (1) (2013) 33–43.
[38] K. Büttner, S. Nehring, K.-P. Hopfner, Structural basis for DNA duplex separation by a superfamily-2 helicase, Nat. Struct. Mol. Biol. 14 (7) (2007) 647–652.
[39] J.D. Richards, K.A. Johnson, H. Liu, A.-M. McRobbie, S. McMahon, M. Oke, L. Carter, J.H. Naismith, M.F. White, Structure of the DNA repair helicase hel308 reveals DNA binding and autoinhibitory domains, J. Biol. Chem. 283 (8) (2008) 5118–5126.
[40] I.M. Derrington, J.M. Craig, E. Stava, A.H. Laszlo, B.C. Ross, H. Brinkerhoff, I. C. Nova, K. Doering, B.I. Tickman, M. Ronaghi, J.G. Mandell, K.L. Gunderson, J. H. Gundlach, Subangstrom single-molecule measurements of motor proteins using a nanopore, Nat. Biotechnol. 33 (10) (2015) 1073–1075.
[41] M. Gu, C.M. Rice, Three conformational snapshots of the hepatitis C virus NS3 helicase reveal a ratchet translocation mechanism, Proc. Natl. Acad. Sci. USA 107 (2) (2010) 521–528.
[42] J.L. Kim, K.A. Morgenstern, J.P. Griffith, M.D. Dwyer, J.A. Thomson, M. A. Murcko, C. Lin, P.R. Caron, Hepatitis C virus NS3 RNA helicase domain with a bound oligonucleotide: the crystal structure provides insights into the mode of unwinding, Structure 6 (1) (1998) 89–100.
[43] E.J. Enemark, L. Joshua-Tor, Mechanism of DNA translocation in a replicative hexameric helicase, Nature 442 (7100) (2006) 270–275.
[44] S.-J. Lee, S. Syed, E.J. Enemark, S. Schuck, A. Stenlund, T. Ha, L. Joshua-Tor, Dynamic look at DNA unwinding by a replicative helicase, Proc. Natl. Acad. Sci. USA 111 (9) (2014) E827–E835.
[45] M.J. Jezewska, S. Rajendran, W. Bujalowski, Complex of *Escherichia coli* primary replicative helicase DnaB protein with a replication fork: Recognition and structure, Biochemistry 37 (9) (1998) 3116–3136.
[46] Y. Gao, Y. Cui, T. Fox, S. Lin, H. Wang, N. de Val, Z.H. Zhou, W. Yang, Structures and operating principles of the replisome, Science 363 (6429) (2019), https://doi.org/10.1126/science:aav7003.
[47] N.D. Thomsen, M.R. Lawson, L.B. Witkowsky, S. Qu, J.M. Berger, Molecular mechanisms of substrate-controlled ring dynamics and substepping in a nucleic acid-dependent hexameric motor, Proc. Natl. Acad. Sci. U. S. A. 113 (48) (2016) E7691–E7700.
[48] N.D. Thomsen, J.M. Berger, Running in reverse: The structural basis for translocation polarity in hexameric helicases, Cell 139 (3) (2009) 523–534.
[49] H.M. Perera, M.A. Trakselis, Amidst multiple binding orientations on fork DNA, *Saccharolobus* MCM helicase proceeds N-first for unwinding, Elife 8 (2019).
[50] R. Georgescu, Z. Yuan, L. Bai, R. de Luna Almeida Santos, J. Sun, D. Zhang, O. Yurieva, H. Li, M.E. O'Donnell, Structure of eukaryotic CMG helicase at a replication fork and implications to replisome architecture and origin initiation, Proc. Natl. Acad. Sci. U. S. A. 114(5) (2017) E697-E706.
[51] M.E. Douglas, F.A. Ali, A. Costa, J.F.X. Diffley, The mechanism of eukaryotic CMG helicase activation, Nature 555 (7695) (2018) 265–268.
[52] J.P. Erzberger, J.M. Berger, Evolutionary relationships and structural mechanisms of AAA^+ proteins, Annu. Rev. Biophys. Biomol. Struct. 35 (1) (2006) 93–114.

[53] D.D. Leipe, L. Aravind, N.V. Grishin, E.V. Koonin, The bacterial replicative helicase DnaB evolved from a RecA duplication, Genome Res. 10 (1) (2000) 5–16.
[54] M.A. Trakselis, Structural mechanisms of hexameric helicase loading, assembly, and unwinding, F1000Research 5 (111) (2016) 1–12.
[55] A.M. Pyle, Translocation and unwinding mechanisms of RNA and DNA helicases, Annu. Rev. Biophys. 37 (1) (2008) 317–336.
[56] Y. Gao, W. Yang, Different mechanisms for translocation by monomeric and hexameric helicases, Curr. Opin. Struct. Biol. 61 (2020) 25–32.
[57] J.M. Berger, SnapShot: Nucleic acid helicases and translocases, Cell 134(5) (2008) 888-888 e1.
[58] O.M. Mazina, M.J. Rossi, J.S. Deakyne, F. Huang, A.V. Mazin, Polarity and bypass of DNA heterology during branch migration of Holliday junctions by human RAD54, BLM, and RECQ1 proteins, J. Biol. Chem. 287 (15) (2012) 11820–11832.
[59] C. Hayashi, E. Miyazaki, S. Ozaki, Y. Abe, T. Katayama, DnaB helicase is recruited to the replication initiation complex via binding of DnaA domain I to the lateral surface of the DnaB N-terminal domain, J. Biol Chem. 295 (32) (2020) 11131–11143.
[60] V.L. O'Shea, J.M. Berger, Loading strategies of ring-shaped nucleic acid translocases and helicases, Curr. Opin. Struct. Biol. 25 (2014) 16–24.
[61] H.M. Perera, M.S. Behrmann, J.M. Hoang, W.C. Griffin, M.A. Trakselis, Contacts and context that regulate DNA helicase unwinding and replisome progression, Enzymes 45 (2019) 183–223.
[62] M.G. Clarey, J.P. Erzberger, P. Grob, A.E. Leschziner, J.M. Berger, E. Nogales, M. Botchan, Nucleotide-dependent conformational changes in the DnaA-like core of the origin recognition complex, Nat. Struct. Mol. Biol. 13 (8) (2006) 684–690.
[63] Y.J. Jeong, V. Rajagopal, S.S. Patel, Switching from single-stranded to double-stranded DNA limits the unwinding processivity of ring-shaped T7 DNA helicase, Nucleic Acids Res. 41 (7) (2013) 4219–4229.
[64] M. Pacek, A.V. Tutter, Y. Kubota, H. Takisawa, J.C. Walter, Localization of MCM2-7, Cdc45, and GINS to the site of DNA unwinding during eukaryotic DNA replication, Mol. Cell 21 (4) (2006) 581–587.
[65] T. Oyama, S. Ishino, T. Shirai, T. Yamagami, M. Nagata, H. Ogino, M. Kusunoki, Y. Ishino, Atomic structure of an archaeal GAN suggests its dual roles as an exonuclease in DNA repair and a CMG component in DNA replication, Nucleic Acids Res. 44 (19) (2016) 9505–9517.
[66] W. Yang, Lessons learned from UvrD helicase: mechanism for directional movement, Annu. Rev. Biophys. 39 (1) (2010) 367–385.
[67] S.S. Patel, I. Donmez, Mechanisms of helicases, J. Biol. Chem. 281 (27) (2006) 18265–18268.
[68] B. Bhattacharyya, J.L. Keck, Grip it and rip it: Structural mechanisms of DNA helicase substrate binding and unwinding, Protein Sci. 23 (11) (2014) 1498–1507.
[69] S.S. Velankar, P. Soultanas, M.S. Dillingham, H.S. Subramanya, D.B. Wigley, Crystal structures of complexes of PcrA DNA helicase with a DNA substrate indicate an inchworm mechanism, Cell 97 (1) (1999) 75–84.
[70] S.G. Mackintosh, K.D. Raney, DNA unwinding and protein displacement by superfamily 1 and superfamily 2 helicases, Nucleic Acids Res. 34 (15) (2006) 4154–4159.
[71] A.K. Byrd, K.D. Raney, Increasing the length of the single-stranded overhang enhances unwinding of duplex DNA by bacteriophage T4 Dda helicase, Biochemistry 44 (39) (2005) 12990–12997.
[72] A.J. Tackett, Y. Chen, C.E. Cameron, K.D. Raney, Multiple full-length NS3 molecules are required for optimal unwinding of oligonucleotide DNA in vitro, J. Biol. Chem. 280 (11) (2005) 10797–10806.
[73] N.K. Maluf, C.J. Fischer, T.M. Lohman, A dimer of *Escherichia coli* UvrD is the active form of the helicase *in vitro*, J. Mol. Biol. 325 (5) (2003) 913–935.
[74] I. Wong, K.L. Chao, W. Bujalowski, T.M. Lohman, DNA-induced dimerization of the *Escherichia coli* rep helicase. Allosteric effects of single-stranded and duplex DNA, J. Biol. Chem. 267 (11) (1992) 7596–7610.
[75] A. Niedziela-Majka, M.A. Chesnik, E.J. Tomko, T.M. Lohman, *Bacillus stearothermophilus* PcrA monomer is a single-stranded DNA translocase but not a processive helicase in vitro, J. Biol. Chem. 282 (37) (2007) 27076–27085.
[76] S. Barranco-Medina, R. Galletto, DNA binding induces dimerization of Saccharomyces cerevisiae Pif1, Biochemistry 49 (39) (2010) 8445–8454.
[77] L.T. Chisty, C.P. Toseland, N. Fili, G.I. Mashanov, M.S. Dillingham, J.E. Molloy, M.R. Webb, Monomeric PcrA helicase processively unwinds plasmid lengths of DNA in the presence of the initiator protein RepD, Nucleic Acids Res. 41 (9) (2013) 5010–5023.
[78] Y.A. Ordabayev, B. Nguyen, A. Niedziela-Majka, T.M. Lohman, Regulation of UvrD helicase activity by MutL, J. Mol. Biol. 430 (21) (2018) 4260–4274.
[79] Y.A. Ordabayev, B. Nguyen, A.G. Kozlov, H. Jia, T.M. Lohman, UvrD helicase activation by MutL involves rotation of its 2B subdomain, Proc. Natl. Acad. Sci. USA 116 (33) (2019) 16320–16325.
[80] M.A. Makurath, K.D. Whitley, B. Nguyen, T.M. Lohman, Y.R. Chemla, Regulation of Rep helicase unwinding by an auto-inhibitory subdomain, Nucleic Acids Res. 47 (5) (2019) 2523–2532.
[81] M. Amaratunga, T.M. Lohman, *Escherichia-coli* Rep helicase unwinds DNA by an active mechanism, Biochemistry 32 (27) (1993) 6815–6820.
[82] T.M. Lohman, Helicase-catalyzed DNA unwinding, J. Biol. Chem. 268 (4) (1993) 2269–2272.
[83] T.M. Lohman, K.P. Bjornson, Mechanisms of helicase-catalyzed DNA unwinding, Annu. Rev. Biochem. 65 (1) (1996) 169–214.
[84] O. Itsathitphaisarn, R. Wing, W. Eliason, J. Wang, T. Steitz, The hexameric helicase DnaB adopts a nonplanar conformation during translocation, Cell 151 (2) (2012) 267–277.
[85] M. Meagher, L.B. Epling, E.J. Enemark, DNA translocation mechanism of the MCM complex and implications for replication initiation, Nat. Commun. 10 (1) (2019) 3117.
[86] P. Eickhoff H.B. Kose F. Martino T. Petojevic F. Abid Ali J. Locke N. Tamberg A. Nans J.M. Berger M.R. Botchan H. Yardimci A. Costa 28 10 2019 2673 2688.e8.
[87] M.D. Betterton, F. Julicher, Opening of nucleic-acid double strands by helicases: Active versus passive opening, Phys Rev. E Stat. Nonlin. Soft Matter Phys. 71 (1 Pt 1) (2005), 011904.
[88] T.M. Lohman, *Escherichia coli* DNA helicases: Mechanisms of DNA unwinding, Mol. Microbiol. 6 (1) (1992) 5–14.
[89] M. Manosas, X.G. Xi, D. Bensimon, V. Croquette, Active and passive mechanisms of helicases, Nucleic Acids Res. 38 (16) (2010) 5518–5526.
[90] P. Soultanas, M.S. Dillingham, P. Wiley, M.R. Webb, D.B. Wigley, Uncoupling DNA translocation and helicase activity in PcrA: Direct evidence for an active mechanism, EMBO J. 19 (14) (2000) 3799–3810.
[91] N.M. Stano, Y.-J. Jeong, I. Donmez, P. Tummalapalli, M.K. Levin, S.S. Patel, DNA synthesis provides the driving force to accelerate DNA unwinding by a helicase, Nature 435 (7040) (2005) 370–373.
[92] S. Kim, H.G. Dallmann, C.S. McHenry, K.J. Marians, Coupling of a replicative polymerase and helicase: A tau-DnaB interaction mediates rapid replication fork movement, Cell 84 (4) (1996) 643–650.
[93] D.S. Johnson, L.u. Bai, B.Y. Smith, S.S. Patel, M.D. Wang, Single-molecule studies reveal dynamics of DNA unwinding by the ring-shaped T7 helicase, Cell 129 (7) (2007) 1299–1309.
[94] L.D. Langston, C. Indiani, M. O'Donnell, Whither the replisome: Emerging perspectives on the dynamic nature of the DNA replication machinery, Cell Cycle 8 (17) (2009) 2686–2691.
[95] L.M. Spenkelink, R.R. Spinks, S. Jergic, J.S. Lewis, N.E. Dixon, A.M. van Oijen, The *E. coli* helicase does not use ATP during replication, bioRxiv (2021) 2021.07.07.451541.
[96] N. Sigal, H. Delius, T. Kornberg, M.L. Gefter, B. Alberts, A DNA-unwinding protein isolated from *Escherichia coli*: Its interaction with DNA and with DNA polymerases, Proc. Natl. Acad. Sci. U. S. A. 69 (12) (1972) 3537–3541.
[97] J.W. Chase, K.R. Williams, Single-stranded-DNA binding-proteins required for DNA-replication, Annu. Rev. Biochem. 55 (1) (1986) 103–136.
[98] J. Kawaoka, E. Jankowsky, A.M. Pyle, Backbone tracking by the SF2 helicase NPH-II, Nat. Struct. Mol. Biol. 11 (6) (2004) 526–530.
[99] P. Ahnert, S.S. Patel, Asymmetric interactions of hexameric bacteriophage T7 DNA helicase with the 5'- and 3'-tails of the forked DNA substrate, J. Biol. Chem. 272 (51) (1997) 32267–32273.
[100] K.J. Hacker, K.A. Johnson, A hexameric helicase encircles one DNA strand and excludes the other during DNA unwinding, Biochemistry 36 (46) (1997) 14080–14087.
[101] D.L. Kaplan, M.J. Davey, M. O'Donnell, Mcm 4,6,7 uses a "pump in ring" mechanism to unwind DNA by steric exclusion and actively translocate along a duplex, J. Biol. Chem. 278 (49) (2003) 49171–49182.
[102] B.W. Graham, G.D. Schauer, S.H. Leuba, M.A. Trakselis, Steric exclusion and wrapping of the excluded DNA strand occurs along discrete external binding paths during MCM helicase unwinding, Nucleic Acids Res. 39 (15) (2011) 6585–6595.
[103] S.M. Carney, S. Gomathinayagam, S.H. Leuba, M.A. Trakselis, Bacterial DnaB helicase interacts with the excluded strand to regulate unwinding, J. Biol. Chem. 292 (46) (2017) 19001–19012.
[104] L. Langston, M. O'Donnell, Action of CMG with strand-specific DNA blocks supports an internal unwinding mode for the eukaryotic replicative helicase, eLife 6 (2017) e23449.
[105] D. Li, R. Zhao, W. Lilyestrom, D. Gai, R. Zhang, J.A. DeCaprio, E. Fanning, A. Jochimiak, G. Szakonyi, X.S. Chen, Structure of the replicative helicase of the oncoprotein SV40 large tumour antigen, Nature 423 (6939) (2003) 512–518.
[106] Y. Chaban, J.A. Stead, K. Ryzhenkova, F. Whelan, E.P. Lamber, A. Antson, C. M. Sanders, E.V. Orlova, Structural basis for DNA strand separation by a hexameric replicative helicase, Nucleic Acids Res. 43 (17) (2015) 8551–8563.
[107] A. Javed, B. Major, J.A. Stead, C.M. Sanders, E.V. Orlova, Unwinding of a DNA replication fork by a hexameric viral helicase, Nat. Commun. 12 (1) (2021) 5535.
[108] L.M. Hellman, M.G. Fried, Electrophoretic mobility shift assay (EMSA) for detecting protein-nucleic acid interactions, Nat. Protoc. 2 (8) (2007) 1849–1861.
[109] B.J. Anderson, C. Larkin, K. Guja, J.F. Schildbach, Using fluorophore-labeled oligonucleotides to measure affinities of protein-DNA interactions, Methods Enzymol. 450 (2008) 253–272.
[110] I. Jarmoskaite, I. AlSadhan, P.P. Vaidyanathan, D. Herschlag, How to measure and evaluate binding affinities, Elife 9 (2020).
[111] S.S. Jain, T.D. Tullius, Footprinting protein-DNA complexes using the hydroxyl radical, Nat. Protoc. 3 (6) (2008) 1092–1100.
[112] A.J. Hampshire, D.A. Rusling, V.J. Broughton-Head, K.R. Fox, Footprinting: A method for determining the sequence selectivity, affinity and kinetics of DNA-binding ligands, Methods 42 (2) (2007) 128–140.
[113] C.A. Davis, M.W. Capp, M.T. Record Jr., R.M. Saecker, The effects of upstream DNA on open complex formation by Escherichia coli RNA polymerase, Proc. Natl. Acad. Sci. U. S. A. 102 (2) (2005) 285–290.
[114] C.T. Bui, K. Rees, R.G. Cotton, Permanganate oxidation reactions of DNA: Perspective in biological studies, Nucleos. Nucleot. Nucl. Acids 22 (9) (2003) 1835–1855.
[115] M. Kato, K. Matsunaga, N. Shimizu, A novel unusual DNA structure formed in an inverted repeat sequence, Biochem. Biophys. Res. Commun. 246 (2) (1998) 532–534.

[116] A.S. Cardew, K.R. Fox, DNase I footprinting, Methods Mol. Biol. 613 (2010) 153–172.
[117] N. Loizos, Mapping protein-ligand interactions by hydroxyl-radical protein footprinting, Methods Mol. Biol. 261 (2004) 199–210.
[118] L.i. Zhang, J.D. Gralla, Micrococcal nuclease as a probe for bound and distorted DNA in lac transcription and repression complexes, Nucleic Acids Res. 17 (13) (1989) 5017–5028.
[119] P.S. Pendergrast, Y. Chen, Y.W. Ebright, R.H. Ebright, Determination of the orientation of a DNA binding motif in a protein-DNA complex by photocrosslinking, Proc. Natl. Acad. Sci. U. S. A. 89 (21) (1992) 10287–10291.
[120] I.M. Nodelman F. Bleichert A. Patel R. Ren K.C. Horvath J.M. Berger G.D. Bowman 65 3 2017 447 459.e6.
[121] J.T. Owens, R. Miyake, K. Murakami, A.J. Chmura, N. Fujita, A. Ishihama, C. F. Meares, Mapping the sigma 70 subunit contact sites on *Escherichia coli* RNA poymerase with a sigma 70 -conjugated chemical protease, Proc. Natl. Acad. Sci. U. S. A. 95 (1998) 6021–6026.
[122] H.M. Perera, M. Trakselis, Site-specific DNA mapping of protein binding orientation using azidophenacyl bromide (APB), Bio-protocol 10 (12) (2020), e3649.
[123] W.-Q. Wu, X.-M. Hou, B.o. Zhang, P. Fossé, B. René, O. Mauffret, M. Li, S.-X. Dou, X.-G. Xi, Single-molecule studies reveal reciprocating of WRN helicase core along ssDNA during DNA unwinding, Sci. Rep. 7 (1) (2017), https://doi.org/10.1038/srep43954.
[124] L. Stryer, Fluorescence energy transfer as a spectroscopic ruler, Annu. Rev. Biochem. 47 (1) (1978) 819–846.
[125] P. Wu, L. Brand, Resonance energy transfer: Methods and applications, Anal. Biochem. 218 (1) (1994) 1–13.
[126] S. Blouin, T.D. Craggs, D.A. Lafontaine, J.C. Penedo, Functional studies of DNA-protein interactions using FRET techniques, Methods Mol. Biol. 1334 (2015) 115–141.
[127] S. Valuchova, J. Fulnecek, A.P. Petrov, K. Tripsianes, K. Riha, A rapid method for detecting protein-nucleic acid interactions by protein induced fluorescence enhancement, Sci. Rep. 6 (2016) 39653.
[128] E.M.S. Stennett, M.A. Ciuba, S. Lin, M. Levitus, Demystifying PIFE: The photophysics behind the protein-induced fluorescence enhancement phenomenon in Cy3, J. Phys. Chem. Lett. 6 (10) (2015) 1819–1823.
[129] J.-y. Liao, Y. Song, Y. Liu, A new trend to determine biochemical parameters by quantitative FRET assays, Acta Pharmacol Sin 36 (12) (2015) 1408–1415.
[130] B.o. Sun, M.D. Wang, Single-molecule perspectives on helicase mechanisms and functions, Crit. Rev. Biochem. Mol. Biol. 51 (1) (2016) 15–25.
[131] X.A. Feng, M.F. Poyton, T. Ha, Multicolor single-molecule FRET for DNA and RNA processes, Curr. Opin. Struct. Biol. 70 (2021) 26–33.
[132] A.T. McGeoch, M.A. Trakselis, R.A. Laskey, S.D. Bell, Organization of the archaeal MCM complex on DNA and implications for the helicase mechanism, Nat. Struct. Mol. Biol. 12 (9) (2005) 756–762.
[133] E. Rothenberg, M.A. Trakselis, S.D. Bell, T. Ha, MCM forked substrate specificity involves dynamic interaction with the 5'-tail, J. Biol. Chem. 282 (47) (2007) 34229–34234.
[134] J.M. Miller, B.T. Arachea, L.B. Epling, E.J. Enemark, Analysis of the crystal structure of an active MCM hexamer, Elife 3 (2014) e03433.
[135] H.e. Song, X. Ji, The mechanism of RNA duplex recognition and unwinding by DEAD-box helicase DDX3X, Nat. Commun. 10 (1) (2019), https://doi.org/10.1038/s41467-019-11083-2.
[136] P. Goswami, F. Abid Ali, M.E. Douglas, J. Locke, A. Purkiss, A. Janska, P. Eickhoff, A. Early, A. Nans, A.M.C. Cheung, J.F.X. Diffley, A. Costa, Structure of DNA-CMG-Pol epsilon elucidates the roles of the non-catalytic polymerase modules in the eukaryotic replisome, Nat. Commun. 9 (1) (2018) 5061.
[137] F. Abid Ali, M.E. Douglas, J. Locke, V.E. Pye, A. Nans, J.F.X. Diffley, A. Costa, Cryo-EM structure of a licensed DNA replication origin, Nat. Commun. 8 (1) (2017) 2241.
[138] A. Costa, I. Ilves, N. Tamberg, T. Petojevic, E. Nogales, M.R. Botchan, J.M. Berger, The structural basis for MCM2-7 helicase activation by GINS and Cdc45, Nat. Struct. Mol. Biol. 18 (4) (2011) 471–477.
[139] M.R. Wasserman, G.D. Schauer, M.E. O'Donnell, S. Liu, Replication fork activation is enabled by a single-stranded DNA gate in CMG helicase, Cell 178 (3) (2019) 600–611.e16.
[140] Y. Noguchi, Z. Yuan, L. Bai, S. Schneider, G. Zhao, B. Stillman, C. Speck, H. Li, Cryo-EM structure of Mcm2-7 double hexamer on DNA suggests a lagging-strand DNA extrusion model, Proc. Natl. Acad. Sci. U. S. A. 114 (45) (2017) E9529–E9538.
[141] R. Ayala, O. Willhoft, R.J. Aramayo, M. Wilkinson, E.A. McCormack, L. Ocloo, D. B. Wigley, X. Zhang, Structure and regulation of the human INO80-nucleosome complex, Nature 556 (7701) (2018) 391–395.
[142] R. Sundaramoorthy, A.L. Hughes, H. El-Mkami, D.G. Norman, H. Ferreira, T. Owen-Hughes, Structure of the chromatin remodelling enzyme Chd1 bound to a ubiquitinylated nucleosome, Elife 7 (2018).
[143] J. Sun Y.i. Shi R.E. Georgescu Z. Yuan B.T. Chait H. Li M.E. O'Donnell The architecture of a eukaryotic replisome 22 12 2015 976 982.
[144] A. Flaus, D.M.A. Martin, G.J. Barton, T. Owen-Hughes, Identification of multiple distinct Snf2 subfamilies with conserved structural motifs, Nucleic Acids Res. 34 (10) (2006) 2887–2905.
[145] I.M. Nodelman, G.D. Bowman, Biophysics of chromatin remodeling, Annu. Rev. Biophys. 50 (1) (2021) 73–93.
[146] J. Winger, G.D. Bowman, The sequence of nucleosomal DNA modulates sliding by the Chd1 chromatin remodeler, J. Mol. Biol. 429 (6) (2017) 808–822.
[147] J. Winger, I.M. Nodelman, R.F. Levendosky, G.D. Bowman, A twist defect mechanism for ATP-dependent translocation of nucleosomal DNA, Elife 7 (2018).
[148] B.T. Harada, W.L. Hwang, S. Deindl, N. Chatterjee, B. Bartholomew, X.W. Zhuang, Stepwise nucleosome translocation by RSC remodeling complexes, Elife 5 (2016).
[149] A. Hada, S.K. Hota, J. Luo, Y.-C. Lin, S. Kale, A.K. Shaytan, S.K. Bhardwaj, J. Persinger, J. Ranish, A.R. Panchenko, B. Bartholomew, Histone octamer structure is altered early in ISW2 ATP-dependent nucleosome remodeling, Cell reports 28 (1) (2019) 282–294.e6.
[150] W. Bujalowski, M.J. Jezewska, Kinetic mechanism of the single-stranded DNA recognition by *Escherichia coli* replicative helicase DnaB protein. Application of the matrix projection operator technique to analyze stopped-flow kinetics, J. Mol. Biol. 295 (4) (2000) 831–852.
[151] A.L. Lucius, C. Jason Wong, T.M. Lohman, Fluorescence stopped-flow studies of single turnover kinetics of *E. coli* RecBCD helicase-catalyzed DNA unwinding, J. Mol. Biol. 339 (4) (2004) 731–750.
[152] C.J. Fischer, E.J. Tomko, C.G. Wu, T.M. Lohman, Fluorescence methods to study DNA translocation and unwinding kinetics by nucleic acid motors, Methods Mol. Biol. 875 (2012) 85–104.
[153] E.J. Tomko, C.J. Fischer, T.M. Lohman, Ensemble methods for monitoring enzyme translocation along single stranded nucleic acids, Methods 51 (3) (2010) 269–276.
[154] M.S. Dillingham, D.B. Wigley, M.R. Webb, Direct measurement of single-stranded DNA translocation by PcrA helicase using the fluorescent base analogue 2-aminopurine, Biochemistry 41 (2) (2002) 643–651.
[155] H. Hwang, H. Kim, S. Myong, Protein induced fluorescence enhancement as a single molecule assay with short distance sensitivity, Proc. Natl. Acad. Sci. U. S. A. 108 (18) (2011) 7414–7418.
[156] H. Hwang, S. Myong, Protein induced fluorescence enhancement (PIFE) for probing protein-nucleic acid interactions, Chem. Soc. Rev. 43 (4) (2014) 1221–1229.
[157] T. Paul, A.F. Voter, R.R. Cueny, M. Gavrilov, T. Ha, J.L. Keck, S. Myong, E., *coli* Rep helicase and RecA recombinase unwind G4 DNA and are important for resistance to G4-stabilizing ligands, Nucleic Acids Res. 48 (12) (2020) 6640–6653.
[158] R. Zhou, J. Zhang, M.L. Bochman, V.A. Zakian, T. Ha, Periodic DNA patrolling underlies diverse functions of Pif1 on R-loops and G-rich DNA, Elife 3 (2014) e02190.
[159] S.J. Lee, S. Syed, T. Ha, Single-molecule FRET analysis of replicative helicases, Methods Mol. Biol. 2018 (1805) 233–250.
[160] Yupeng Qiu, Robert F. Levendosky, Srinivas Chakravarthy, Ashok Patel, Gregory D. Bowman, Sua Myong, The Chd1 chromatin remodeler shifts nucleosomal DNA bidirectionally as a monomer, Mol. Cell 68 (1) (2017) 76–88.e6.
[161] E. Lerner, A. Barth, J. Hendrix, B. Ambrose, V. Birkedal, S.C. Blanchard, R. Borner, H.S. Chung, T. Cordes, T.D. Craggs, A.A. Deniz, J.J. Diao, J.Y. Fei, R. L. Gonzalez, I.V. Gopich, T. Ha, C.A. Hanke, G. Haran, N.S. Hatzakis, S. Hohng, S. C. Hong, T. Hugel, A. Ingargiola, C. Joo, A.N. Kapanidis, H.D. Kim, T. Laurence, N.K. Lee, T.H. Lee, E.A. Lemke, E. Margeat, J. Michaelis, X. Michalet, S. Myong, D. Nettels, T.O. Peulen, E. Ploetz, Y. Razvag, N.C. Robb, B. Schuler, H. Soleimaninejad, C. Tang, R. Vafabakhsh, D.C. Lamb, C.A.M. Seidel, S. Weiss, FRET-based dynamic structural biology: Challenges, perspectives and an appeal for open-science practices, Elife 10 (2021).
[162] Samar Hodeib, Saurabh Raj, Maria Manosas, Weiting Zhang, Debjani Bagchi, Bertrand Ducos, Francesca Fiorini, Joanne Kanaan, Hervé Le Hir, Jean-François Allemand, David Bensimon, Vincent Croquette, A mechanistic study of helicases with magnetic traps, Protein Sci. 26 (7) (2017) 1314–1336.
[163] B. Sun, M.D. Wang, Single-molecule optical-trapping techniques to study molecular mechanisms of a replisome, Methods Enzymol. 582 (2017) 55–84.
[164] C.T. Lin, T. Ha, Direct visualization of helicase dynamics using fluorescence localization and optical trapping, Methods Enzymol. 582 (2017) 121–136.
[165] Z.H. Qin, L.L. Bin, X.M. Hou, S.Q. Zhang, X. Zhang, Y. Lu, M. Li, M. Modesti, X. G. Xi, B. Sun, Human RPA activates BLM's bidirectional DNA unwinding from a nick, Elife 9 (2020).
[166] Thomas C.R. Miller, Julia Locke, Julia F. Greiwe, John F.X. Diffley, Alessandro Costa, Mechanism of head-to-head MCM double-hexamer formation revealed by cryo-EM, Nature 575 (7784) (2019) 704–710.
[167] James R. Kiefer, Chen Mao, Jeffrey C. Braman, Lorena S. Beese, Visualizing DNA replication in a catalytically active *Bacillus* DNA polymerase crystal, Nature 391 (6664) (1998) 304–307.
[168] Yang Gao, Wei Yang, Capture of a third Mg(2)(+) is essential for catalyzing DNA synthesis, Science 352 (6291) (2016) 1334–1337.
[169] Venkata P. Dandey, William C. Budell, Hui Wei, Daija Bobe, Kashyap Maruthi, Mykhailo Kopylov, Edward T. Eng, Peter A. Kahn, Jenny E. Hinshaw, Nidhi Kundu, Crina M. Nimigean, Chen Fan, Nattakan Sukomon, Seth A. Darst, Ruth M. Saecker, James Chen, Brandon Malone, Clinton S. Potter, Bridget Carragher, Time-resolved cryo-EM using spotiton, Nat. Methods 17 (9) (2020) 897–900.
[170] J. Frank, Time-resolved cryo-electron microscopy: Recent progress, J. Struct. Biol. 200 (3) (2017) 303–306.
[171] Jonathan M. Craig, Andrew H. Laszlo, Henry Brinkerhoff, Ian M. Derrington, Matthew T. Noakes, Ian C. Nova, Benjamin I. Tickman, Kenji Doering, Noah F. de Leeuw, Jens H. Gundlach, Revealing dynamics of helicase translocation on single-stranded DNA using high-resolution nanopore tweezers, Proc. Natl. Acad. Sci. U. S. A. 114 (45) (2017) 11932–11937.
[172] Thomas D. Pollard, Douglas Kellogg, A guide to simple and informative binding assays, Mol. Biol. Cell 21 (23) (2010) 4061–4067.